Food Hydrocolloids 134 (2023) 108009

Contents lists available at ScienceDirect

Food Hydrocolloids

journal homepage: www.elsevier.com/locate/foodhyd

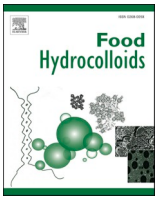

Tribology and rheology of water-in-water emulsions stabilized by whey protein microgels

Kwan-Mo You, Brent S. Murray, Anwesha Sarkar *

Food Colloids and Bioprocessing Group, School of Food Science and Nutrition, University of Leeds, Leeds, LS2 9JT, United Kingdom

ARTICLE INFO

Keywords:
Starch
Carrageenan
Whey protein microgel
Friction
Lubrication
Rheology

ABSTRACT

This study aimed to investigate the microstructural, tribological and rheological properties of water-in-water (W/W) emulsion droplets with or without stabilization by proteinaceous microgel particles. The W/W emulsions were prepared from mixtures of gelatinized corn starch (GS) and κ-carrageenan (κC) in the two-phase regime and when particle-stabilized whey protein microgel particles (WPM) were used. The W/W emulsions were shear thinning liquids. The viscosity values of the emulsions were higher than the corresponding weight average values, calculated on individual samples irrespective of shear rates. Tribological results revealed that the frictional properties of W/W emulsions formed from 1.0 wt% GS + 0.1 w% κC were dominated by the κC properties alone in the mixed and hydrodynamic regimes, even though the starch played an essential role in decreasing friction coefficient (μ) in the boundary regime. Unlike the corresponding solutions of GS and κC, W/W emulsions containing higher concentrations of the biopolymers (3.0 wt% starch + 0.3 wt% κC) decreased μ in the mixed and boundary regimes, probably due to water droplets becoming entrained and forming a hydration film in the contact region. In the case of W/W emulsions containing WPM, confocal and cryo-scanning electron microscopy confirmed the presence of WPM at the interface and hence a Pickering-like stabilization. The WPM-stabilized W/W emulsions showed higher apparent viscosity (than those without WPM) and lower μ in the boundary and mixed regimes. Stabilization of W/W emulsions via microgel particles therefore seems to be a useful tool to improve the lubrication performance of such systems.

1. Introduction

Water-in-water (W/W) emulsions are thermodynamically incompatible solutions of two biopolymers (Esquena, 2016; Hazt et al., 2020; Nicolai & Murray, 2017; Vis, Opdam, et al., 2015). Such emulsions demonstrate phase separation, producing water droplets much richer in one biopolymer dispersed in a continuous phase much richer in the other biopolymer. The degree and rate of phase separation are associated with the molecular weight of the biopolymers and any charge interaction between the polymer segments. (Grinberg & Tolstoguzov, 1997; Nicolai & Murray, 2017). Since W/W emulsions evolve from a 'mixed' solution, they start off, at least in the early stages of their formation, with a much larger interfacial area in the system as compared to that of oil-in-water (O/W) or water-in-oil (W/O) emulsion systems formed by mechanical dispersions of one immiscible phase into the other. Furthermore, the interfacial tensions of W/W emulsions (*e.g.*, $<10^{-2}$ mM m^{-1}) are orders of magnitude smaller than those of O/W emulsions (*e.g.*, 30 mM m^{-1}) (Ding et al., 2002; Scholten, Visser, Sagis, & van der Linden, 2004; Vis et al., 2015a, 2015b; Vis et al., 2015a, 2015b). Recently, there has been increasing interest in using surface active particles to stabilize W/W emulsions (Esquena, 2016). A wide range of proteinaceous microgel particles, for example, using β-lactoglobulin, whey protein isolate (WPI), bovine serum albumin (BSA) and gelatin, have been used (Beldengrun et al., 2018; Hazt et al., 2020; Machado, Capron, de Freitas, Benyahia, & Nicolai, 2022; Murray & Phisarnchananan, 2014, 2016; Zhang et al., 2021).

Although the design principles and formulation strategies of W/W emulsions have been well-researched (Esquena, 2016; Murray & Ettelaie, 2020), the interaction of W/W emulsions with bodily fluids has attracted little attention to date. In particular, very little is known about the oral behavior of W/W emulsions, which is crucial if such emulsions are to be used in food applications. Oral processing involves a dynamic range of deformation in a relatively short span of time that can be assessed using rheological and tribological analysis to understand the bulk and surface effects, respectively (Chen & Stokes, 2012; Sarkar, Andablo-Reyes, Bryant, Dowson, & Neville, 2019). There is now a

* Corresponding author.
E-mail address: A.Sarkar@leeds.ac.uk (A. Sarkar).

https://doi.org/10.1016/j.foodhyd.2022.108009
Received 25 February 2022; Received in revised form 8 July 2022; Accepted 23 July 2022
Available online 6 August 2022

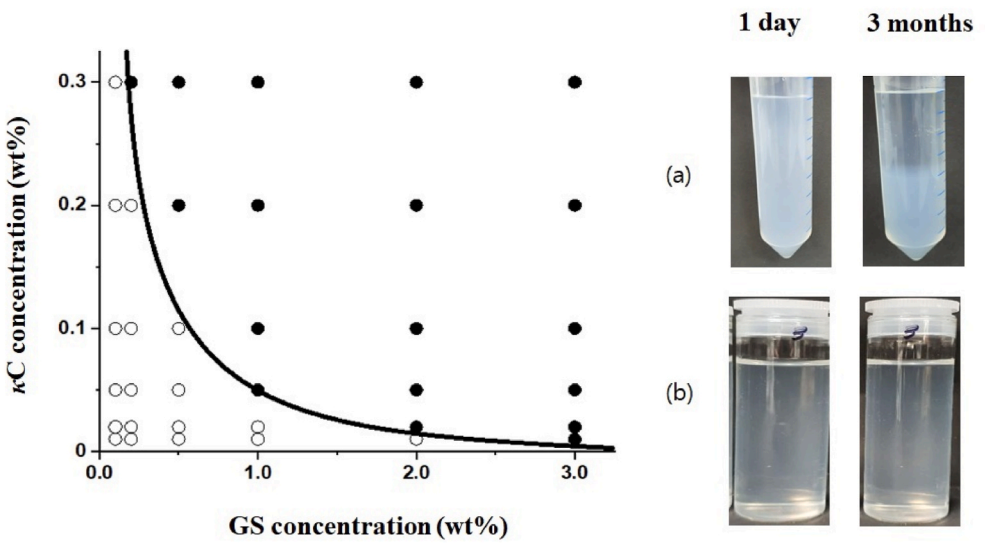

Fig. 1. Phase diagram showing the estimated binodal (–) single-phase (○) and biphasic (●) mixtures of gelatinized waxy corn starch (S) and κ-carrageenan (κC) with visual images of (a) 2.0 wt% GS + 0.2 wt% κC, and (b); 0.25 wt% GS + 0.5 wt% κC immediately and after a storage period of 3 months.

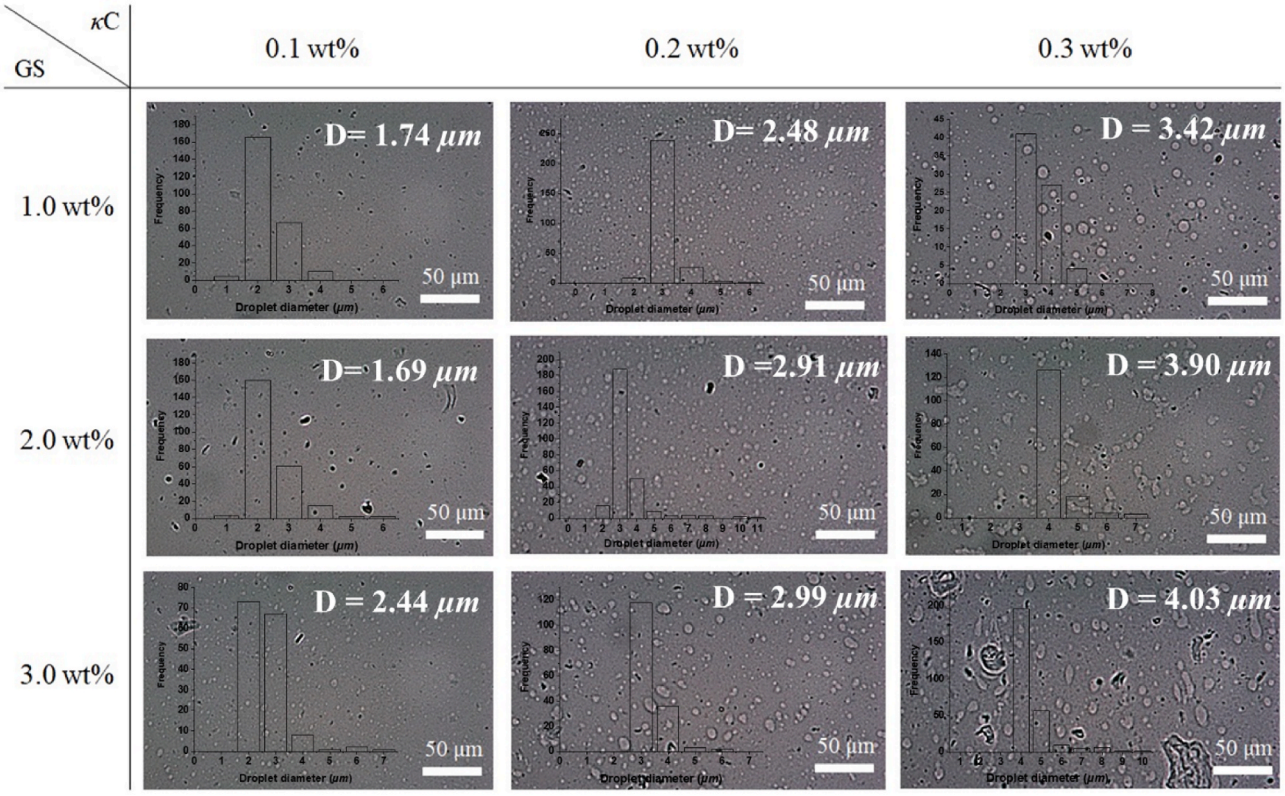

Fig. 2. Optical micrographs of water droplets inside GS + κC phase separating W/W emulsions prepared with different concentrations of GS (1.0–3.0 wt%) and κC (0.1–0.3 wt%) with insets showing histogram of droplet size distribution and mean droplet size of W/W emulsion droplets. Using optical microscopy images of at least 100 droplets, the actual mean droplet size of the W/W emulsions was assessed using ImageJ. Scale bars represent 50 μm.

consensus that bulk effects dominate oral processing in the early stages - affecting sensory perception such as 'thickness' - whereas surface-driven tribological effects dominate the oral processing in the later stages – affecting smoothness, slipperiness *etc.* (Sarkar & Krop, 2019; Stokes, Boehm, & Baier, 2013). Many previous studies have shown the difference in the bulk rheological behavior of W/W emulsions compared with that of the individual constituent biopolymer solutions (Firoozmand, Murray, & Dickinson, 2007; Semenova & Dickinson, 2010; Vis, Opdam, et al., 2015).

In terms of tribology, there has been significant progress in the frictional analysis of emulsions, microgels, emulsion microgels in the last decade (Sarkar, Soltanahmadi, Chen, & Stokes, 2021; Torres, Andablo-Reyes, Murray, & Sarkar, 2018; Upadhyay & Chen, 2019). Upadhyay and Chen (2019) demonstrated that oil volume fraction and droplet size in an O/W emulsion could affect smoothness perception via decreasing the friction coefficient (μ). According to Torres et al. (2018),

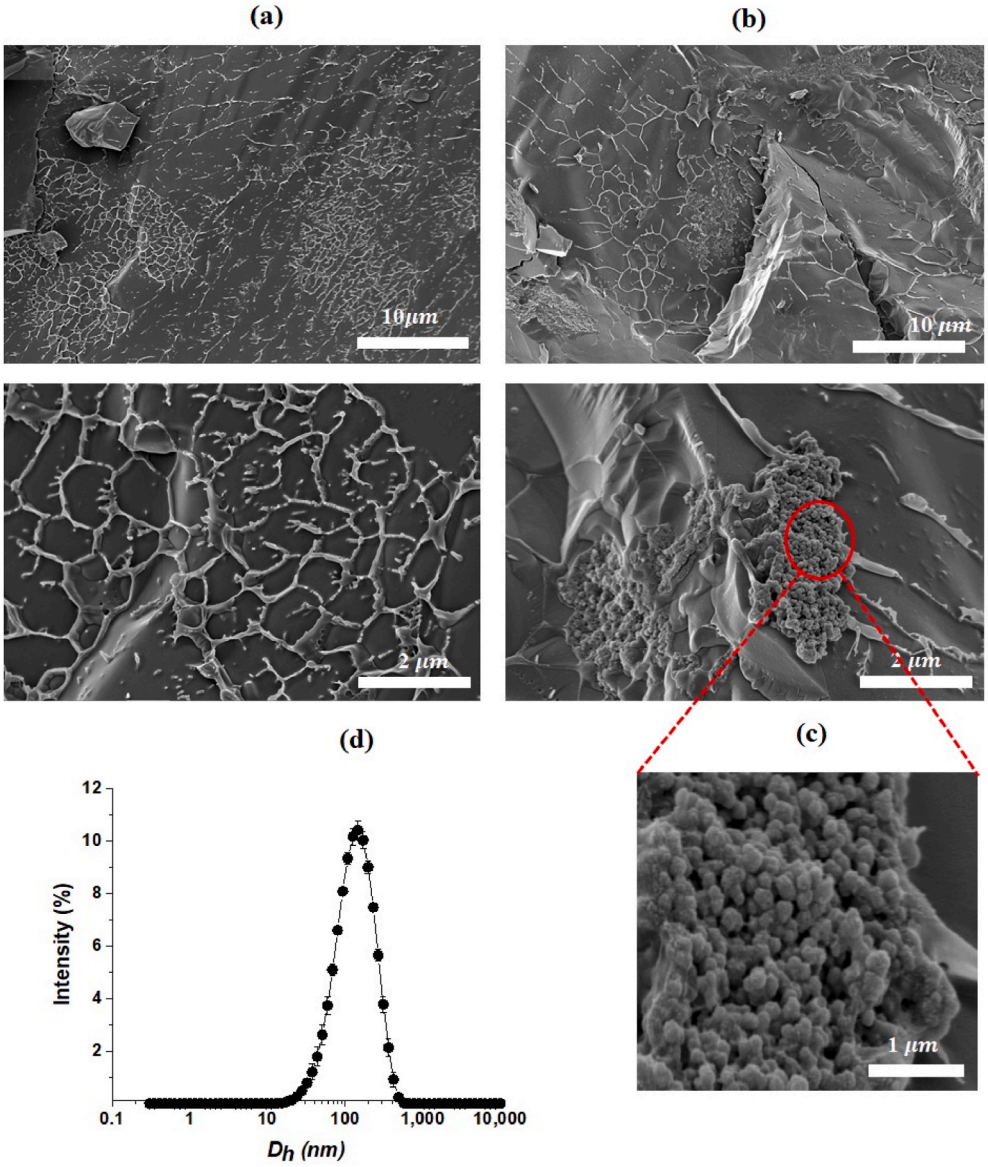

Fig. 3. Cryo-SEM images of 3.0 wt% GS + 0.3 wt% κC W/W emulsions (a) in the absence of whey protein microgel particles (WPM) and (b) in the presence of WPM, with top image showing 20,000 × magnification (scale bar = 10 μm) and bottom image showing 50,000 × magnification (scale bar = 2 μm). Zoomed image of the interface containing WPM (c), and hydrodynamic size (d) of WPM particles measured using dynamic light scattering.

the lubrication performance of O/W emulsions is strongly dependent on the coalescence stability of the droplets and they also highlighted that emulsions stabilized by modified starch can help to reduce μ further by being responsive to α-amylase in mouth. Although there is some understanding of the tribological performance of mixtures of starch and non-starch polysaccharides (You, Murray, & Sarkar, 2021; You & Sarkar, 2021), no study has yet investigated the tribological performance of W/W emulsions that can evolve from such mixtures. Interestingly, the stability of W/W emulsions can be modified by incorporating proteinaceous microgel particles, which pin to the interface via the Pickering mechanism despite the low interfacial tension, whilst at the same time it is already known that such microgels themselves can impact the lubrication performance (Andablo-Reyes et al., 2019; Sarkar, Kanti, Gulotta, Murray, & Zhang, 2017). It remains to be seen if the rheological and tribological properties of such W/W emulsions are dominated by the presence of stable W/W droplets, the microgels or the individual biopolymer solutions.

Consequently, the aim of this study was to form W/W emulsion droplets by combining solutions of gelatinized starch (GS) and κ-carrageenan (κC) with or without whey protein microgel particles (WPM) as droplet stabilizer and to assess their rheological and tribological properties. We mapped the phase diagram and measured the shear viscosity and tribology of κC and GS separately and also when present together as W/W emulsions with and without WPM. We hypothesize that W/W emulsions should reduce μ mostly via accretion of water droplets under the tribological stress into a hydration layer between the tribological contact surface. To our knowledge, this is the first report that investigates the frictional properties of W/W emulsion systems with and without the addition of Pickering-like microgel particles. The findings should bring new knowledge to aid the design of low calorie products without compromising their mouthfeel.

2. Material and methods

2.1. Materials

κ-carrageenan (κC), product code 22048 (CAS number 11114-20-8), and waxy corn starch, product code 10120 (CAS number 9037-22-3)

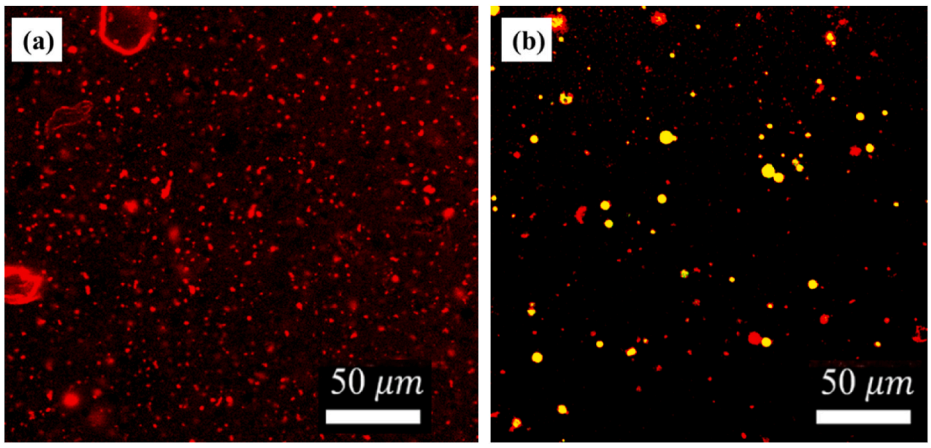

Fig. 4. Confocal micrographs of the 3 wt% GS + 0.3 wt% κC W/W emulsion (a) in the absence and (b) in the presence of whey protein microgel (WPM). GS and WPM are fluorescently labelled by Rhodamine B (λ ≈ 546 nm) and Acridine Orange (λ ≈ 502 nm), respectively. Scar bar represents 50 μm. (For interpretation of the references to colour in this figure legend, the reader is referred to the Web version of this article.)

were purchased from Sigma-Aldrich, Dorset, UK. Biopolymer solutions were made in 20 mM phosphate buffer at pH 7.0. Smooth polydimethylsiloxane materials with a surface roughness of 50 nm (PDMS, Sylgard 184, Dow Corning, USA) tribo-set (ball; ∅ 47 mm, disk; ∅ 19 mm and 4 mm thickness) were purchased from PCS Instruments, London, UK. Rhodamine B (product code R-6626) and Acridine Orange (Product code 15855) were purchased from Sigma Aldrich, Dorset, UK. Phosphate buffer was made up with water purified by a Milli-Q apparatus (Millipore, Bedford, UK), with an electrical resistivity not less than 18.2 MΩ cm.

2.2. Preparation of W/W emulsions

Gelatinized starch (GS) (0.2–6.0 wt%) was prepared by dispersing the starch powder in phosphate buffer at pH 7.0 followed by thermal treatment in an oil bath at 90 °C for 15 min with constant shearing using an Ultra Turrax T25 homogenizer (IKA-Werke GmbH &Co., Staufen Germany) to gelatinize the starch. κ-carrageenan (κC) (0.02–0.6 wt%) was dispersed in phosphate buffer at pH 7.0 for at least 24 h at room temperature and then similarly dispersed and heated at 90 °C for 15 min. Equal volumes of GS and κC solutions of different concentrations were mixed at 90 °C and homogenized at 21,000 rpm for 10 min via the Ultra Turrax T25 homogenizer. For Pickering W/W emulsions stabilized by microgel particles, the microgel particles (0.1–1.5 vol% in the final mixture) were added to either the GS or κC solutions before blending the two phases together.

2.3. Preparation of whey protein isolate microgel particles (WPM)

The WPM were prepared using the procedure described in previous reports (Andablo-Reyes et al. (2019); Sarkar et al. (2017)). Briefly, whey protein isolate (WPI) solution was prepared by dissolving 12.0 g WPI in 88.0 g of 20 mM phosphate buffer at pH 7.0 and stirred for 2 h at room temperature to ensure complete dissolution. Crosslinking to form a WPI gel was achieved by heating the WPI solution at 90 °C for 30 min. After cooling to room temperature the gel was stored at 4 °C for 12 h, followed by blending for 2 min with 20 mM phosphate buffer, at a 1:5 w/w ratio of gel to buffer, via a hand blender (HB711M, Kenwood, UK). The subsequent dispersion of 'coarse' WPI gel fragments was degassed via a THINKY mixer (ARE-250, Kidlington, UK) using a mixing cycle of 2 min at 2000 rpm, followed by 1 min degassing at 2200 rpm. Finally, the dispersion of fragments was formed into a fine dispersion of WPM via two passes through a bespoke Jet Homogenizer (University of Leeds, UK) at 300 ± 20 bar. The final concentration of WPM particles in the GS or κC dispersions to form the W/W emulsions (see above) was 20.0 vol% (equivalent to 2.4 wt% protein).

2.4. Dynamic light scattering

The particle size of the WPM was measured via dynamic light scattering (DLS) using a Zetasizer (Nano ZS series, Malvern Instruments, Worcestershire, UK). A sample of the WPM dispersion was diluted with 20 mM phosphate buffer solution at a 1: 50 v/v ratio of WPM to buffer and placed in a disposable plastic cuvette (ZEN 0040). Measurements were performed by time-dependent correlation functions, using a detection angle of 173° and refractive indices of 1.54 and 1.33 for WPM and buffer, respectively. The absorbance of the WPM particles was assumed to be 0.001.

2.5. Apparent viscosity

Rheological characterization of the biopolymer solutions and W/W emulsions was performed via a model MCR 302 (Anton Paar, Austria) shear rheometer, using cone-and-plate geometry (CP50-2, cone diameter 50 mm, cone angle 2°, 1 mm gap) at shear rates ranging from 0.1 to 1000 s^{-1}. All the experiments were carried out within 2 h of W/W emulsion formation, during which time no visible phase separation of the emulsions occurred. For each measurement, 2 mL of sample were pipetted onto the plate and a temperature-controlled cover was used to prevent evaporation and maintain the temperature at 37 ± 0.1 °C, in order to mimic oral processing conditions. Samples were left on the plate for 2 min to achieve thermal equilibrium before rheological measurements commenced.

2.6. Tribology

A Mini Traction Machine 2 (MTM2, PCS Instruments, London, UK) with hydrophobic polydimethylsiloxane (PDMS) ball and disc as tribo-pairs, was used to measure the tribological performance of the samples. All the experiments were carried out within 2 h of W/W emulsion formation. A normal load (*W*) of 2 N and a slide-to-roll ratio (*SRR*) of 50% were used for all frictional measurements. The friction coefficients were measured for all samples as a function of entrainment speed (*U*); sliding speeds were varied from 1 to 1000 mm s^{-1}. The temperature was controlled at 37 ± 1 °C. The friction coefficients are reported below as the mean and standard deviation of at least three measurements carried out on triplicate samples prepared on different days.

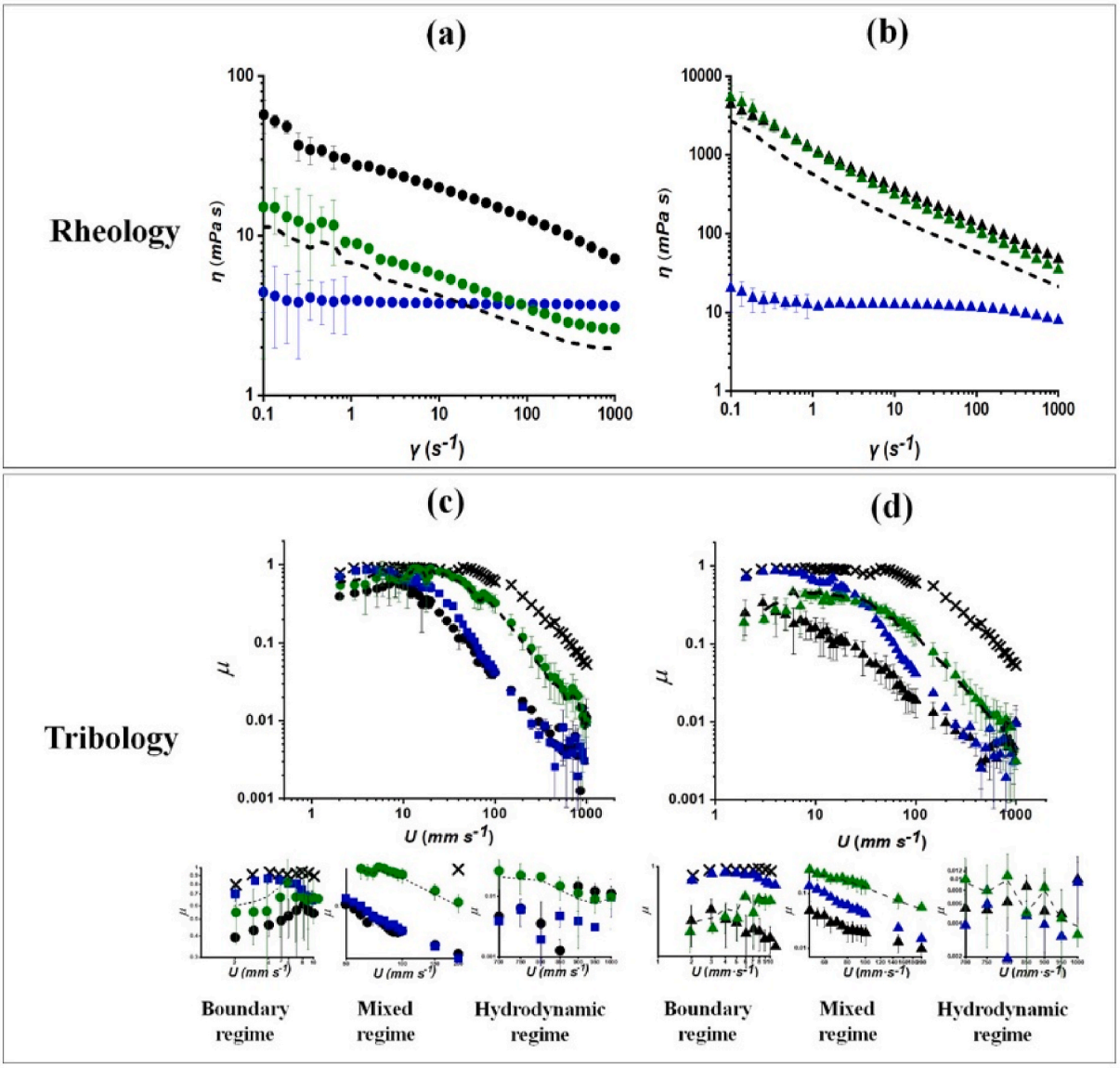

Fig. 5. Mean apparent viscosity (η) as a function of shear rate (γ) (a, b) and mean friction coefficient (μ) versus entrainment speed (U) (c, d) of W/W emulsions without the addition of WPM; (a and c) 1.0 wt% GS (●), 0.1 wt% κC (●), and (b and d) 3.0 wt% GS (▲), 0.3 wt% κC (▲), and W/W emulsions (●; 1.0 wt% GS + 0.1 wt % κC, ▲; 3.0 wt% GS + 0.3 wt% κC). The weight average values of the corresponding individual controls for the mixtures are also shown (–), and phosphate buffer is used as a control (×). Error bars represent standard deviations. The images in the bottom show the zoomed version of (c) and (d) each lubrication regime. (For interpretation of the references to colour in this figure legend, the reader is referred to the Web version of this article.)

2.7. Phase diagram via imaging of the W/W emulsions

Freshly prepared W/W emulsions were stored at 25 °C in flat bottom test tubes sealed with a plastic cap and photographed periodically to establish the 1 or 2 phase regions of the phase diagram as a function of composition.

2.8. Microscopy

Optical microscopy (Nikon, SMZ-2T, Japan) was used to observe the microstructure of the W/W emulsions with different concentrations of GS and κC with 40× magnification lens. ImageJ software (version 1.48r, National Institute of Health, Bethesda, USA) was used to determine the diameter of the emulsion droplets and the mean droplet size was calculated using at least 100 droplets in multiple images.

Confocal scanning laser microscopy (CLSM) of blends was performed using a Leica TCS SP2 confocal laser scanning microscope (Leica Microsystems, Manheim Germany) connected with a Leica Model DM RXE microscope base. The confocal was used with Ar/ArKr (488, 514 nm) and He/Ne (543, 633 nm) laser sources. Laser excitation of the fluorescent samples was at 514 nm (≈ 29% intensity of laser) for Rhodamine Blue (RB) and 488 nm (≈ 49% intensity of laser) for Acridine Orange (AO). A 20 × objective with numerical aperture 0.5 was used to obtain all images, at 1024 × 1024 pixel resolution. 0.5 wt% of RB and 0.5 wt% AO were dissolved with MilliQ water and the solutions were stored in the dark when not being used. For mixtures without WPM particles, 30 μL of the RB solution was added per 5 mL of the GS solution before blending with κC. For the S + κC blends with WPM particles, 30 μL of the AO solution were added per 5 mL of gum phase before blending. After blending the mixtures via the Ultra Turrax, samples without added WPM particles were immediately poured into a welled slide 30 mm diameter and 0.3 mm in depth. RB showed preferential staining of GS whilst the cationic AO showed strong affinity for the WPM particles. Unlabelled areas were therefore assumed to be the κC-rich

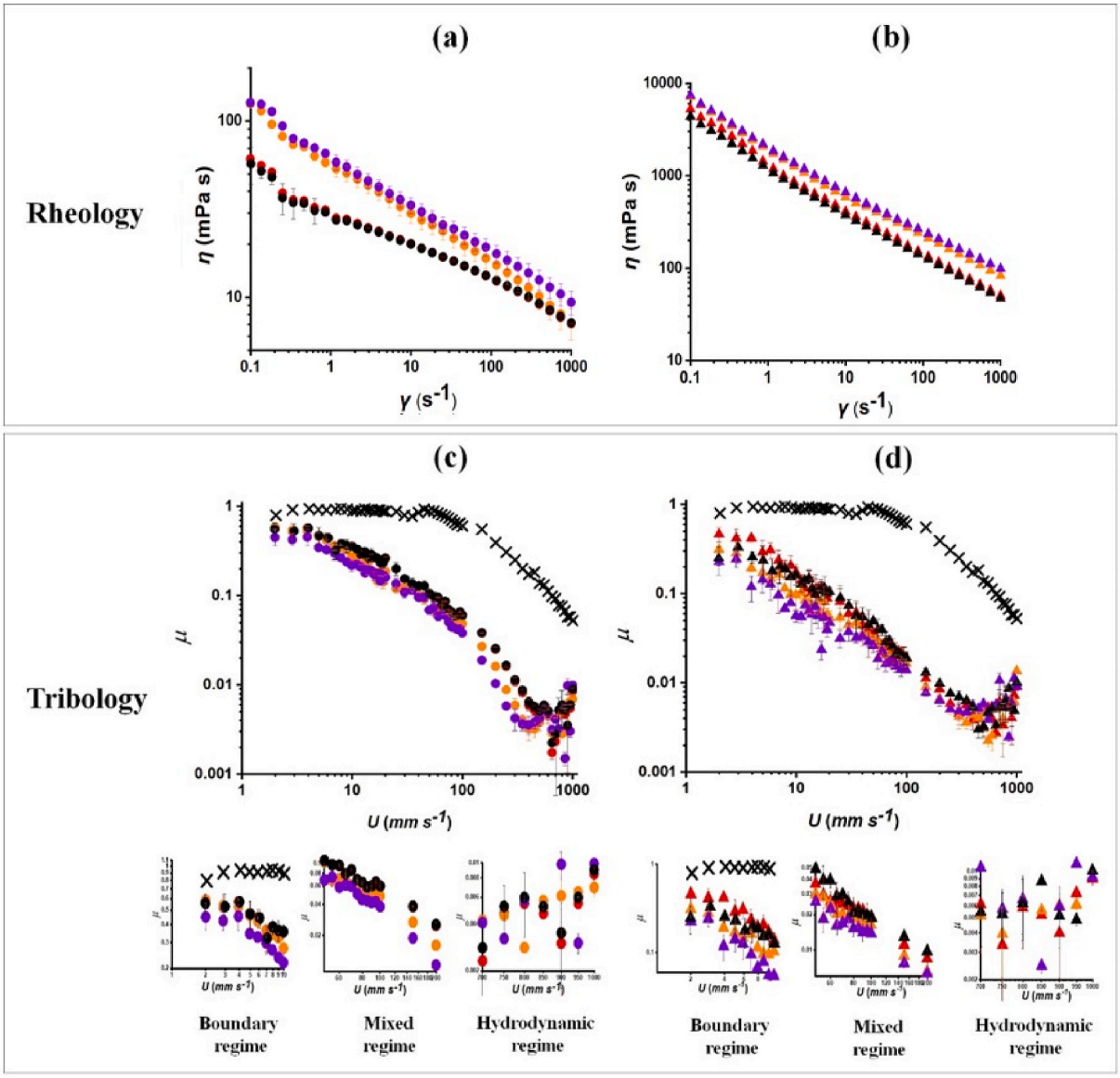

Fig. 6. Apparent viscosity (η) as a function of shear rate (γ) (a, b) and friction coefficient (μ) versus entrainment speed (U) (c, d) of W/W emulsions with the addition of WPM; at (a and c) lower biopolymer concentrations (1.0 wt% GS and 0.1 wt% κC, ●) and (b and d) higher biopolymer concentrations (3.0 wt% GS and 0.3 wt% κC, ▲) with different concentration of WPM; 0.5 vol% (●, ▲), 1.5 vol% (●, ▲), and 3.0 vol% (●, ▲). Phosphate buffer is used as a control (×). Error bars represent standard deviations. The images in the bottom show the zoomed version of (c) and (d) each lubrication regime. (For interpretation of the references to colour in this figure legend, the reader is referred to the Web version of this article.)

regions. The first image was captured 5 min after blending the mixtures. For systems containing WPM particles, it was necessary to wait for 20 min to allow any air bubbles to rise out of the samples before they could be poured into the welled slide and the cover slip added. The appearance of samples was recorded 0.5–24 h after creating the W/W emulsions.

Cryogenic scanning electron microscopy (cryo-SEM) of the W/W emulsions was also conducted. The samples were mounted on rivets attached to the sample stub. The samples were plunge-frozen in liquid nitrogen "slush" at −180 °C, then transferred to the cryo-preparation chamber on the SEM. The samples were then cleaved and etched at −95 °C for 4 min, followed by coating with 5 nm of platinum (Pt). Finally, the Pt-coated samples were transferred to the SEM chamber for imaging at −135 °C.

2.9. Statistical analysis

All experimental results are presented the mean and standard deviation of at least three measurements on triplicate samples (n = 3 × 3). Statistical analyses were carried out for tribological data at boundary regimes (5–10 mm s^{-1}), mixed regimes (100–150 mm s^{-1}) and hydrodynamic regimes (700–900 mm s^{-1}) using one-way ANOVA and multiple comparison test via SPSS software and differences between samples were deemed significantly different with $p < 0.05$ via Tukey's test.

3. Results and discussion

3.1. Phase diagram

Published phase diagrams in literature appear to vary, even using the same biopolymers, due to the wide range of conformation of macromolecules from different sources, batches, *etc.* (Capron, Costeux, & Djabourov, 2001). The phase diagram for our samples of GS and κC is shown in Fig. 1. After three months of quiescent storage under normal gravity, phase separation was confirmed with the formation of an

Table 1
Means and standard deviations (SDs) of friction coefficient the W/W emulsions in the absence of WPM; 1.0 wt% GS + 0.1 wt% κC and 3.0 wt% GS and 0.3 wt% κC, and in the presence of 0.5–3.0 vol% WPM in each boundary, mixed, and hydrodynamic regimes. Different lower case letters in the same column indicate a statistically significant difference ($p < 0.05$).

(a) Friction coefficient of 1.0 wt% GS + 0.1 wt% κC emulsions without or with WPM

	Boundary lubrication regime (5–10 mm s^{-1})		Mixed lubrication regime (100–150 mm s^{-1})		Hydrodynamic lubrication regime (700–900 mm s^{-1})	
	Mean	SD	Mean	SD	Mean	SD
no added WPM	0.550[a]	0.0373	0.049 [a]	0.0083	0.0085[a]	0.0018
0.5 vol% WPM	0.390[a]	0.0513	0.048[b]	0.0109	0.0059[b]	0.0018
1.5 vol% WPM	0.365[ab]	0.0617	0.038[c]	0.0108	0.0056[c]	0.0015
3.0 vol% WPM	0.283[ac]	0.0459	0.029[d]	0.0096	0.0060[d]	0.0034

(b) Friction coefficient of 3.0 wt% GS + 0.3 wt% κC emulsions without or with WPM

	Boundary lubrication regime (5–10 mm s^{-1})		Mixed lubrication regime (100–150 mm s^{-1})		Hydrodynamic lubrication regime (700–900 mm s^{-1})	
	Mean	SD	Mean	SD	Mean	SD
no added WPM	0.178[a]	0.0320	0.016[a]	0.0029	0.0070[a]	0.0020
0.5 vol% WPM	0.235[b]	0.0493	0.015[b]	0.0041	0.0063[b]	0.0017
1.5 vol% WPM	0.132[c]	0.0306	0.013[c]	0.0037	0.0075[c]	0.0031
3.0 vol% WPM	0.095[d]	0.0313	0.011[d]	0.0031	0.0071[d]	0.0030

opaque lower (GS-rich) phase and a more clear upper (κC-rich) phase, similar to that determined previously by Murray and Phisarnchananan (2014) for GS-locust bean gum and GS-guar gum systems. Further measurements (not shown) for longer times showed that phase separation was still not entirely complete for those systems where two phases were already visible after storage for three months. The rate of phase separation was slower at higher concentrations of κC and/or GS, as expected due to the increased viscosity of the κC and GS phases, which is discussed later.

It can be seen that the binodal line lies close to GS concentration axis and very close to the κC concentration axis at low GS but higher κC (Fig. 1). At higher concentrations of GS (1.0, 2.0 and 3.0 wt%), the mixtures were all biphasic at κC concentrations up to the lowest concentration studied (0.05 wt %). The critical polymer concentration (CPC) in which phase separation could be observed at the 50:50 wt% line was 0.75:0.075 (GS: κC). Below this value, there was no visible macroscopic difference in turbidity of the mixtures in the tubes, and so it was assumed that no phase separation occurred (*i.e.*, one phase, no W/W emulsions formed). Note that, 'immediately' (<15 min) after their formation, all the mixtures appeared homogeneous by visual observation.

3.2. W/W emulsion microstructure without and with WPM

Above the CPC after 15 min, W/W droplets could be observed via optical microscopy in the 1.0 wt% GS + 0.1 wt% κC system, with different sizes and shapes of water droplets (Fig. 2). The concentration of GS appeared to affect the size of the droplets, with the smallest droplets visible in the 1.0 wt% GS + 0.1 wt% κC system and the droplets becoming larger with increasing concentration of GS, from 1.7 μm to 2.44 μm diameter of water droplets at the same κC concentration, whereas the largest droplets were observed at 3.0 wt% GS + 0.3 wt% κC system. Interestingly, κC seemed to affect the shape of the W/W droplets. At lower κC concentrations (0.1 wt%), the water droplets were more spherical, whilst they appeared to be oval-shaped at higher concentrations (*e.g.*, 0.3 wt% κC + 3.0 wt% GS). It is possible to control W/W droplet size by modulating the shear rate (Stokes, Wolf, & Frith, 2001) during phase separation. For example, Stokes, et al. (2001) showed 7 μm droplets at a shear rate between two parallel plates of 100 s^{-1} but 30 μm at shear rates of 10 s^{-1}. Differences in shape affect the W/W interfacial area and, therefore the overall free energy of the system, spheres minimizing this, of course. The final morphology is dependent on temperature, molecular ordering and the relative phase volume of the equilibrium phases (Esquena, 2016; Shewan & Stokes, 2013) and consequently, many different W/W droplet structures are inherently unstable. Butler and Heppenstall-Butler (2003) demonstrated bicontinuous structures in biopolymer mixtures whilst decreasing the temperature accelerated spinodal decomposition. Non-spherical structures can also be kinetically trapped by crosslinking the dispersed phase (Shewan & Stokes, 2013). In summary, a wide range of shapes can be expected (spheres, ellipsoids, rods, and fibrils), depending on the exact combination of polymer samples, conditions of phase separation and whether or not there is any material that can preferentially adsorb at the W–W interface (Murray & Phisarnchananan, 2016; Turgeon, Schmitt, & Sanchez, 2007; Wolf, Scirocco, Frith, & Norton, 2000).

Cryogenic scanning electron microscopy (Cryo-SEM) observations at lower length scales (Fig. 3) show separation of the samples into polyhedral aqueous regions, which may therefore be the water droplets that have become distorted during the preparation. In the presence of WPM (Fig. 3b and c), and in particular in the zoomed in region of Fig. 3c, there appear to be particles at the interstices of the polyhedral regions. Fig. 3d shows the particle size distribution of the WPM particles alone, measured via DLS, that shows a strong peak at a hydrodynamic diameter (d_H) = 115 ± 3 nm. This size seems to correspond well to the interstitial particles, although clearly they might be quite aggregated (Fig. 3c), but suggests that a major fraction of the WPM do collect at the W–W interface. To our knowledge, limited study has shown cryo-SEM evidence of WPM at the interface of W/W emulsion droplets, although, many cryo-SEM studies have shown WPM at the oil-water interface of oil-in-water (O/W) emulsions (Destribats, Rouvet, Gehin-Delval, Schmitt, & Binks, 2014; Sarkar et al., 2017). In these studies, similar kind of interfacial aggregation of WPM is observed as in Fig. 3c.

CLSM micrographs of the W/W emulsions are shown in Fig. 4a and b. In Fig. 4a, in the absence of the WPM, coalescence of droplets (the darker, unstained regions) is suggested. In Fig. 4b, in the presence of WPM, stained with Acridine Orange (AO), numerous spherical objects can be observed, much smaller than the dark aqueous regions in Fig. 4a (where no WPM is present). These spherical regions in Fig. 4b are uniformly stained with AO, suggesting that they are W/W droplets coated in WPM, again demonstrating the ability of WPM to act as the Pickering-like particles necessary for stabilizing W/W emulsion systems (Beldengrun et al., 2018; Esquena, 2016; Hazt et al., 2020; Vis, Opdam, et al., 2015). There are many studies that have discussed how the pH can be tuned to induce protein microgel particles to adsorb at the W–W interface more effectively and reduce the size of the discontinuous phase regions in W/W systems (de Freitas, Nicolai, Chassenieux, & Benyahia, 2016; Hazt et al., 2020). However, the objective of our study was to understand the behavior under oral processing conditions, hence the pH was kept at 7.0 and pH variations were not pursued further.

3.3. Rheological and tribological characteristics

3.3.1. W/W emulsions without WPM

Fig. 5a and Fig. 5b show apparent viscosity (η) of the W/W emulsions prepared using lower (1.0 wt% GS + 0.1 wt% κC) and higher (3.0 wt% GS + 0.3 wt% κC) biopolymer concentrations, respectively, alongside controls of same concentrations of GS and κC alone. These emulsions were prepared without WPM. Rheologically speaking, the W/W emulsions, regardless of concentration, were different to either κC or GS, and have non-Newtonian behavior, with shear-thinning properties. The apparent viscosity η of the W/W emulsions decreased by at least one order and two orders of magnitude for the lower (1.0 wt% GS + 0.1 wt% κC) and higher (3.0 wt% GS + 0.3 wt% κC) biopolymer concentrations, respectively (Fig. 5a and Fig. 5b) in the shear rate experimental window covering a range from 0.1 to 1000 s^{-1}. It is noteworthy that η, irrespective of the biopolymer concentration, did not show the onset of the

second Newtonian plateau - making it not possible to scale the experimental tribology data with viscosity.

The dashed lines in Fig. 5a and b are the calculated weighted averages of the individual equilibrium phases (GS and κC) and are dominated by the GS, since the concentration of GS is 10 × higher than that of κC. Particularly for the lower biopolymer concentrations, η for the emulsions was significantly higher than these average values at the corresponding shear rates. At the higher biopolymer concentrations (3.0 wt% GS + 0.3 wt% κC), there was some convergence at the lowest shear rate measured (1 s^{-1}). Apart from the κC solutions alone (0.1 or 0.3 wt%), all systems were also significantly shear thinning, only 0.1 wt% GS showed some tendency to level off at high shear rates of 1000 s^{-1}. There are many studies that show that the viscosity of biopolymer mixtures including κC tends to be higher than that of κC alone (Fakharian et al., 2015; Huc et al., 2014; Lafargue et al., 2007) as in our case. This is usually explained by some sort of attractive interaction between GS and κC (for example via hydrogen bonding between the hydroxyl groups on the polysaccharides). In the case of the emulsions without WPM, as seen in Fig. 4a, there appeared to be coalescence of the droplets (presumably preceded by aggregation), which might also contribute to enhanced viscosity of the emulsions compared to the individual biopolymers. In addition, any increasing volume fraction of dispersed phase will increase the viscosity of the continuous phase. In these systems it is hard to estimate what this volume fraction might be at any instant, since it evolves with time as the phase separation proceeds.

In the case of the tribology data, Fig. 5c and d illustrate the friction coefficient (μ) as a function of entrainment speed (U) of the W/W emulsions with lower and higher biopolymer concentrations, respectively, whilst the corresponding controls for the GC and κC alone are also shown, along with that of the phosphate buffer. The buffer shows boundary and mixed lubrication regimes but no hydrodynamic regime until $U \approx 1000$ mm s^{-1}. The boundary regime is maintained at $\mu \approx 1.0$, and then a decrease in μ is observed as a function of increasing U. Such a prolonged boundary regime with phosphate buffer has been observed previously as phosphate buffer is squeezed out of the hydrophobic PDMS-PDMS contact zone (Sarkar et al., 2017; You et al., 2021). The tribological behavior of the W/W emulsion at the lower biopolymer concentrations (1.0 wt% GS + 0.1 wt% κC) was similar to that reported previously by You et al. (2021), where either κC or GS dominates in the different regimes. In the boundary regime GS dominates, whilst in the mixed and hydrodynamic regimes the W/W emulsion behavior increasingly seems to follow the signature of the κC alone. At the higher concentrations (3.0 wt% GS + 0.3 wt% κC) in the boundary and mixed regimes the W/W emulsion had a lower μ than the corresponding GS and κC solutions alone (Fig. 5d). We explain this as due to the water droplets becoming entrained and forming a hydration film in the contact region. As noted earlier (Fig. 2), the water droplets appear to have different sizes, morphologies and also volume fractions, depending on the biopolymer concentrations. The higher concentrations seem to give more droplets, larger droplets and droplets with more non-spherical shapes, whereas the lower concentrations seem to give fewer droplets, smaller droplets but droplets with more spherical shapes.

3.3.2. W/W emulsions with WPM

WPM was observed using cryo-SEM and confocal microscopy at the interface of the two phases (Figs. 3b and 4b). The WPM adsorbed at the interface could affect the structure of emulsion system, by increasing the viscosity (Destribats et al., 2014; Sarkar et al., 2017; Zhu, Bhandari, & Prakash, 2019).

In the case of Pickering W/W emulsions, *i.e.*, those W/W systems with added WPM, Fig. 6a and b show their bulk rheological behavior. A significant increase in η was observed on addition of WPM at 1.5 and 3.0 vol%, the increases being rather similar, whereas addition at 0.5 vol% WPM did not have a significant effect on η. Similar effects were observed at both the higher and lower biopolymer concentrations, although all the viscosities were much higher in the latter. Interestingly, the systems were shear-thinning with no high shear rate plateauing effect being observed even at 1000 s^{-1} shear rates.

The presence of WPM did affect the tribological results, in particular in the lubrication regime (see Fig. 6c and d and Table 1). At the lower biopolymer concentrations (Fig. 6c), by increasing the WPM concentrations from 0.5 to 3.0 vol%, μ did not change in the boundary regime ($p < 0.05$). However, it did decrease in the mixed and hydrodynamic regimes: even though the reduction was small it was statistically significant ($p < 0.05$). At the higher biopolymer concentrations (Fig. 6d), the emulsions showed a rather similar trend but the reduction in μ was significant even in the boundary regime ($p < 0.05$) upon addition of >0.5 vol% WPM. Irrespective of the biopolymer concentrations and WPM volume fractions (1.5–3.0 vol% WPM), μ ranged from 0.01 to 0.05 in the mixed regimes in the presence of W/W emulsions containing WPM (Table 1). This might be expected, given the increase in bulk viscosity on addition of WPM (see above), and therefore an improvement in the fluid film lubrication behavior (Andablo-Reyes et al., 2019). However, another possibility is that the WPM-coated W/W emulsion droplets were stable and rolled into the contact zone more effectively, as compared to the droplets without WPM (Table 1). Interestingly, μ increased in the boundary regime on adding 0.5 vol% WPM (Table 1). Sarkar et al. (2017) also showed that low volume fractions of WPM gave relatively poor lubrication properties because the WPM particles could not sufficiently replenish the contact region with particles and overcome the adhesion of PDMS-PDMS surfaces. Thus, the presence of WPM improved the stability of droplets but did not show a decrease in boundary lubrication property at low volume fractions. We suppose that: (i) there was not a high enough volume fraction of WPM particles to lower μ in the boundary regime, and (ii) the pressure in the contact region between the PDMS tribopairs was high enough to exclude such low volume fraction of WPM as well as WPM-coated droplets from the interface. In summary, one should note that although WPM had some statistically significant effects in reducing μ, the absolute reduction was not dramatic in the presence of WPM in the W/W emulsion droplets, as compared to its absence (Table 1). This might be attributed to the amount of WPM used in this study to stabilize the droplets. Increasing the concentration of WPM might be investigated in future work to see if such an increase results in systematic decreases in μ, particularly in the boundary regime.

4. Conclusions

In this study, we demonstrated for the first time the tribological properties of W/W emulsions formed from mixtures of GS and κC with or without added WPM. Different sizes and shapes of the droplets were observed in different parts of the two-phase region of the phase diagram via microscopy across various length scales. The W/W emulsions were shear thinning liquids, with viscosity values being much higher than the corresponding weight average of the values of the individual components. The morphology of the water droplets appeared to affect the rheological and tribological performance. In the case of Pickering-like W/W emulsion droplets, with WPM acting as the stabilizing particles, the apparent bulk viscosity of the W/W emulsions stabilized by particles was significantly higher than that of the corresponding mixtures in the absence of WPM. Interestingly, although there was reduction in boundary lubrication performance with WPM - particularly in W/W emulsion droplets with higher biopolymer concentrations - WPM appeared to produce a significant reduction in friction coefficient in the mixed regimes at higher volume fractions of WPM. Future studies are ongoing to understand the oral processing behavior of these emulsions in presence of saliva to understand whether the presence of the particles allows a more gradual breakdown of the water droplets as the starch in the system is hydrolyzed, as opposed to a more burst release in the absence of WPM, and how this affects tribological performance and mouthfeel.

Credit author statement

Kwan Mo-You: Validation, Formal analysis, Investigation, Data curation, Writing- Reviewing & Editing; Visualization; Writing- Original draft preparation, Writing- Reviewing & Editing, Prof. Brent S. Murray: Conceptualization, Methodology, Supervision, Writing- Reviewing & Editing; Prof. Anwesha Sarkar: Conceptualization, Methodology, Project administration; Writing- Reviewing & Editing, Supervision, Funding acquisition.

Declaration of competing interest

The authors declare that they have no known competing financial interests or personal relationships that could have appeared to influence the work reported in this paper.

Data availability

Data will be made available on request.

Acknowledgement

Funding from the European Research Council (ERC) under the European Union's Horizon 2020 research and innovation programme (grant agreement n° 757993) is acknowledged.

References

Andablo-Reyes, E., Yerani, D., Fu, M., Liamas, E., Connell, S., Torres, O., et al. (2019). Microgels as viscosity modifiers influence lubrication performance of continuum. *Soft Matter, 15*(47), 9614–9624.

Beldengrun, Y., Aragon, J., Prazeres, S. F., Montalvo, G., Miras, J., & Esquena, J. (2018). Gelatin/maltodextrin water-in-water (w/w) emulsions for the preparation of cross-linked enzyme-loaded microgels. *Langmuir, 34*(33), 9731–9743.

Butler, M. F., & Heppenstall-Butler, M. (2003). Phase separation in gelatin/dextran and gelatin/maltodextrin mixtures. *Food Hydrocolloids, 17*(6), 815–830.

Capron, I., Costeux, S., & Djabourov, M. (2001). Water in water emulsions: Phase separation and rheology of biopolymer solutions. *Rheologica Acta, 40*(5), 441–456.

Chen, J., & Stokes, J. R. (2012). Rheology and tribology: Two distinctive regimes of food texture sensation. *Trends in Food Science & Technology, 25*(1), 4–12.

Destribats, M., Rouvet, M., Gehin-Delval, C., Schmitt, C., & Binks, B. P. (2014). Emulsions stabilized by whey protein microgel particles: Towards food-grade pickering emulsions. *Soft Matter, 10*(36), 6941–6954.

Ding, P., Wolf, B., Frith, W., Clark, A., Norton, I., & Pacek, A. (2002). Interfacial tension in phase-separated gelatin/dextran aqueous mixtures. *Journal of Colloid and Interface Science, 253*(2), 367–376.

Esquena, J. (2016). Water-in-water (W/W) emulsions. *Current Opinion in Colloid & Interface Science, 25*, 109–119.

Fakharian, M.-H., Tamimi, N., Abbaspour, H., Nafchi, A. M., & Karim, A. A. (2015). Effects of κ-carrageenan on rheological properties of dually modified sago starch: Towards finding gelatin alternative for hard capsules. *Carbohydrate Polymers, 132*, 156–163. In this issue https://doi.org/10.1016/j.carbpol.2015.06.033.

Firoozmand, H., Murray, B. S., & Dickinson, E. (2007). Fractal-type particle gel formed from gelatin+ starch solution. *Langmuir, 23*(8), 4646–4650.

de Freitas, R. A., Nicolai, T., Chassenieux, C., & Benyahia, L. (2016). Stabilization of water-in-water emulsions by polysaccharide-coated protein particles. *Langmuir, 32*(5), 1227–1232.

Grinberg, V. Y., & Tolstoguzov, V. (1997). Thermodynamic incompatibility of proteins and polysaccharides in solutions. *Food Hydrocolloids, 11*(2), 145–158.

Hazt, B., Bassani, H. P., Elias-Machado, J. P., Buzzo, J. L. A., Silveira, J. L., & de Freitas, R. A. (2020). Effect of pH and protein particle shape on the stability of amylopectin–xyloglucan water-in-water emulsions. *Food Hydrocolloids, 104*, Article 105769.

Huc, D., Matignon, A., Barey, P., Desprairies, M., Mauduit, S., Sieffermann, J.-M., & Michon, C. (2014). Interactions between modified starch and carrageenan during pasting. *Food Hydrocolloids, 36*, 355–361.

Lafargue, D., Lourdin, D., & Doublier, J.-L. (2007). Film-forming properties of a modified starch/κ-carrageenan mixture in relation to its rheological behaviour. *Carbohydrate Polymers, 70*(1), 101–111. https://doi.org/10.1016/j.carbpol.2007.03.019.

Machado, J. P., Capron, I., de Freitas, R. A., Benyahia, L., & Nicolai, T. (2022). Stabilization of amylopectin-pullulan water in water emulsions by Interacting protein particles. *Food Hydrocolloids, 124*, Article 107320.

Murray, B. S., & Ettelaie, R. (2020). Chapter 5. Bijel Systems Based on the Phase Separation of Biological Macromolecules. In P. Clegg (Ed.), *Bijels : Bicontinuous Particle-stabilized Emulsions* (pp. 114–136). London, UK: RSC. In this issue.

Murray, B. S., & Phisarnchananan, N. (2014). The effect of nanoparticles on the phase separation of waxy corn starch+ locust bean gum or guar gum. *Food Hydrocolloids, 42*, 92–99.

Murray, B. S., & Phisarnchananan, N. (2016). Whey protein microgel particles as stabilizers of waxy corn starch+ locust bean gum water-in-water emulsions. *Food Hydrocolloids, 56*, 161–169.

Nicolai, T., & Murray, B. (2017). Particle stabilized water in water emulsions. *Food Hydrocolloids, 68*, 157–163.

Sarkar, A., Andablo-Reyes, E., Bryant, M., Dowson, D., & Neville, A. (2019). Lubrication of soft oral surfaces. *Current Opinion in Colloid & Interface Science, 39*, 61–75.

Sarkar, A., Kanti, F., Gulotta, A., Murray, B. S., & Zhang, S. (2017). Aqueous lubrication, structure and rheological properties of whey protein microgel particles. *Langmuir, 33*(51), 14699–14708.

Sarkar, A., & Krop, E. M. (2019). Marrying oral tribology to sensory perception: A systematic review. *Current Opinion in Food Science, 27*, 64–73.

Sarkar, A., Soltanahmadi, S., Chen, J., & Stokes, J. R. (2021). Oral tribology: Providing insight into oral processing of food colloids. *Food Hydrocolloids, 117*, Article 106635.

Scholten, E., Visser, J. E., Sagis, L. M., & van der Linden, E. (2004). Ultralow interfacial tensions in an aqueous phase-separated gelatin/dextran and gelatin/gum Arabic system: A comparison. *Langmuir, 20*(6), 2292–2297.

Semenova, M. G., & Dickinson, E. (2010). *Biopolymers in food colloids: Thermodynamics and molecular interactions*. CRC Press.

Shewan, H. M., & Stokes, J. R. (2013). Review of techniques to manufacture micro-hydrogel particles for the food industry and their applications. *Journal of Food Engineering, 119*(4), 781–792.

Stokes, J. R., Boehm, M. W., & Baier, S. K. (2013). Oral processing, texture and mouthfeel: From rheology to tribology and beyond. *Current Opinion in Colloid & Interface Science, 18*(4), 349–359.

Stokes, J. R., Wolf, B., & Frith, W. (2001). Phase-separated biopolymer mixture rheology: Prediction using a viscoelastic emulsion model. *Journal of Rheology, 45*(5), 1173–1191.

Torres, O., Andablo-Reyes, E., Murray, B. S., & Sarkar, A. (2018). Emulsion microgel particles as high-performance bio-lubricants. *ACS Applied Materials and Interfaces, 10*(32), 26893–26905.

Turgeon, S., Schmitt, C., & Sanchez, C. (2007). Protein–polysaccharide complexes and coacervates. *Current Opinion in Colloid & Interface Science, 12*(4–5), 166–178.

Upadhyay, R., & Chen, J. (2019). Smoothness as a tactile percept: Correlating 'oral'tribology with sensory measurements. *Food Hydrocolloids, 87*, 38–47.

Vis, M., Opdam, J., Van't Oor, I. S., Soligno, G., Van Roij, R., Tromp, R. H., et al. (2015a). Water-in-water emulsions stabilized by nanoplates. *ACS Macro Letters, 4*(9), 965–968.

Vis, M., Peters, V. F., Blokhuis, E. M., Lekkerkerker, H. N., Erné, B. H., & Tromp, R. H. (2015b). Decreased interfacial tension of demixed aqueous polymer solutions due to charge. *Physical Review Letters, 115*(7), Article 078303.

Vis, M., Peters, V. F., Blokhuis, E. M., Lekkerkerker, H. N., Erné, B. H., & Tromp, R. H. (2015c). Effects of electric charge on the interfacial tension between coexisting aqueous mixtures of polyelectrolyte and neutral polymer. *Macromolecules, 48*(19), 7335–7345.

Wolf, B., Scirocco, R., Frith, W., & Norton, I. (2000). Shear-induced anisotropic microstructure in phase-separated biopolymer mixtures. *Food Hydrocolloids, 14*(3), 217–225.

You, K., Murray, B. S., & Sarkar, A. (2021). Rheology and tribology of starch+ κ-carrageenan mixtures. *Journal of Texture Studies, 52*(1), 16–24.

You, K., & Sarkar, A. (2021). Oral tribology of polysaccharides. In *Handbook of hydrocolloids* (pp. 93–124). Elsevier.

Zhang, J., Mei, L., Ma, P., Li, Y., Yuan, Y., Zeng, Q.-Z., et al. (2021). Microgel-stabilized hydroxypropyl methylcellulose and dextran water-in-water emulsion: Influence of pH, ionic strength, and temperature. *Langmuir, 37*(18), 5617–5626.

Zhu, Y., Bhandari, B., & Prakash, S. (2019). Tribo-rheology characteristics and microstructure of a protein solution with varying casein to whey protein ratios and addition of hydrocolloids. *Food Hydrocolloids, 89*, 874–884.